Miscibility of Poly(vinyl chloride) Melts Composed of Mixtures of Chains with Differing Stereochemical Composition and Stereochemical Sequence

Thomas C. Clancy and Wayne L. Mattice*

Institute of Polymer Science, The University of Akron, Akron, Ohio 44325-3909

Received March 15, 2001; Revised Manuscript Received June 18, 2001

ABSTRACT: Simulations of coarse-grained models of poly(vinyl chloride) (PVC) on a high coordination lattice have been performed for seven pure melts and 12 binary mixtures composed of chains with seven different stereochemical compositions and stereochemical sequences, at a temperature of 450 K and a density of 1.24−1.26 g/cm^3. The same Lennard-Jones parameters are used for all pairs of monomer units in all of the simulations. The chains differ only in their short-range intramolecular interactions, which are controlled by a rotational isomeric state model for PVC. The melt of syndiotactic PVC is unique in that its intermolecular pair correlation functions (pcf) show a greater tendency for the formation of local "structure" than is evident in the simulations of the other polymers, all of which contain *meso* diads. The effect of stereochemistry on demixing properties is investigated by simulation of 12 equimolar binary mixtures. The seven binary mixtures that do not contain syndiotactic PVC remain miscible throughout the simulations. However, all but one of the five binary mixtures containing syndiotactic PVC experience demixing during the simulations. The single exception is the binary mixture of syndiotactic PVC with chains in which the sequence of diads has the repeating pattern *meso*−*racemo*−*racemo*−*racemo*. In this system, the intermolecular pcfs suggest the formation of a weak complex between the chains.

Introduction

The common atactic poly(vinyl chloride) (aPVC) of commerce is a glassy material at ordinary temperatures. For several decades,[1−3] it has been known that this amorphous glass contains a small amount (on the order of 10%) of a more ordered structure. This structure, which causes aPVC to sometimes be described as semicrystalline, has been the subject of investigation using numerous techniques, such as DSC,[4] NMR,[4] SANS,[5,6] SAXS,[2,5] and TMA.[5] Runs of *racemo* diads have been implicated in the formation of this structure.[4] The crystalline regions in plasticized material have been reported to be subject to thermoreversible melting at temperatures of about 80−90 °C.[6] When the PVC has a very high content of *racemo* diads, the thermal transition can be displaced to temperatures above 200 °C, i.e., to temperatures above the limit of thermal stability.[7,8] In the stereochemical limit provided by the syndiotactic PVC (sPVC) prepared in a urea inclusion complex, where the narrow channel presumably precludes the formation of *meso* diads, the polymer becomes intractable.[1,4,9]

Our interest here is in the behavior of PVC at the upper end of the range of temperatures at which the material retains resistance to thermal degradation, i.e., at temperatures slightly below 200 °C. On one hand, we seek information about whether the miscibility of the melts at such temperatures depends on the stereochemical composition and stereochemical sequence of the chains from which they are constructed. Furthermore, in view of the intractable nature of the material prepared in the urea inclusion complex, we inquire whether there is a possibility to design a chain that will promote miscibility of aPVC and sPVC in the melt.

Prior simulations of atomistically detailed models of amorphous aPVC at bulk density have focused on either models for the material at ambient temperature, where the density is 1.39 g/cm^3,[10,11] or models for the melt, with a density of 1.24 g/cm^3.[12] These simulations employed either a single parent chain of 76[10,11] or 200[10] monomer units or 30 shorter parent chains of 12 monomer units each.[12] The restriction to systems of 76−360 monomer units in these previous studies was imposed by the difficulty in thoroughly equilibrating the dense models when they are expressed at fully atomistic detail.

The present simulations employ either 550 monomer units (for one-component systems) or 1000 monomer units (for multicomponent sytems). These larger systems become tractable for simulation when the models are expressed with coarse-grained chains. The coarse-grained chains retain contact with reality, because the coarse graining is accomplished with restrictions that allow reverse mapping back to atomistically detailed models.[13] This objective is accomplished with a bridging technique.[14] The simulation has recently been applied successfully to polypropylene (PP) melts,[15] where it correctly identifies their observed dependence of miscibility on stereochemical composition: aPP and iPP are miscible in the melt, but sPP demixes from either iPP or aPP in the melt.[16−19] Furthermore, the simulation identifies the molecular mechanism responsible for the demixing of sPP from the other two PPs in their melts.[15] It seems likely that this mechanism may apply also to PVC melts, and the present simulations will assess whether this suggestion is correct.

Method

Only a single type of monomer unit, CH_2CHCl, is present in the simulations reported here. Some of the differences in the stereochemical sequences of the chains lead to a tendency for demixing, but other systems composed of two different types of chains are completely miscible. Equilibration of these dense systems would appear to require use of a coarse-grained model, because demixing (when it occurs) is in response to a subtle interaction. However, it is the influence of the stereochemical composition and stereochemical sequence of the chains that is at issue, and those properties are defined in

10.1021/ma010462c CCC: $20.00
Published on Web 08/03/2001

terms of atomistically detailed models. Therefore, it is essential that the coarse-grained models faithfully represent the stereochemical compositions and sequences of the atomistically detailed chains that they represent.

This objective can be achieved with coarse graining at the level of one bead per monomer unit, with that bead sited at the coordinates of the carbon atom that bears the chlorine atom. With standard bond lengths and tetrahedral bond angles, the chain of beads requires a step length of 2.50 Å. The coarse-grained chains are placed on a high-coordination ($10i^2 + 2$ sites in shell i) lattice obtained by deletion of every second site from a diamond lattice.[20] The simulations are performed at low occupancies of 13.16−13.43%, corresponding to densities of 1.24−1.26 g/cm^3. These densities are within a few percent of the expectation of 1.29 g/cm^3, based on linear extrapolation of data tabulated by Orwoll[21] to the temperature of the simulation, 450 K, and comparable with the density of 1.26 g/cm^3 used previously by Smith et al.[12] in their simulations of aPVC at the same temperature.

The distribution function for the end-to-end distance of a chain, and all of its subchains, is controlled by mapping the classic rotational isomeric state (RIS) model for chains with bonds subject to asymmetric torsion potential energy functions onto this lattice.[22] The specific RIS model used in the present simulation is the same one employed in our recent study of single unperturbed PVC chains.[23] This use of the RIS model maintains the initially assigned stereochemical sequence of each chain throughout the simulation.

The intermolecular and long-range intramolecular interactions are treated with a procedure that uses Meyer *f* functions, with input in the form of a Lennard-Jones (LJ) potential energy function.[24] The LJ parameters tabulated for PVC are $\epsilon/k_B = 300$ K and $\sigma = 4.898$ Å.[25] This procedure yields discrete energies (kJ/mol) of 21.968, 1.575, −1.369, −0.468, and −0.124 for shells 1−5, respectively, at the temperature of the simulation, 450 K. Only shells 1−3 are used in the simulation to calculate the change in energy, ΔE, of a proposed MC move for Metropolis biasing. The first shell is highly repulsive because the lattice spacing, 2.50 Å, is smaller than the σ in the LJ potential energy function. The second shell is slightly repulsive, and an anisotropic perturbation is included in this shell. The third shell is attractive and will allow for a cohesive simulated structure. The fourth shell still shows an appreciable attractive interaction, but the computation slows dramatically when it is included in the simulation. To apply the model to PVC, an asymmetric perturbation based on the electrostatic influence of the partial charge on the chlorine atom was added to the second shell interaction, as described previously.[26] This perturbation has the effect of changing the energy of the second shell from ∼−3 to ∼+6 kJ/mol, depending on the orientation of the monomer.

The original single bead MC algorithm for simulations on this lattice consisted of the attempted move of every bead of every chain in sequential fashion, subject to the constraints of connectivity, excluded volume, and Metropolis energetic biasing.[20] In the simulations presented here, multiple bead moves are included as well, as described in a previous publication.[25] All multiple bead moves are constrained to excluded volume, connectivity, and Metropolis energetic biasing. Each chain goes through a cycle of attempted single bead moves and multiple bead moves. After each chain in the system has gone through this cycle, we count one MC "time" step.

Results and Discussion

One-Component Melts. Seven one-component melts were simulated, using 11 independent parent chains, each with a degree of polymerization of 50 and a composition of $C_{100}H_{152}Cl_{50}$ upon reverse mapping. The temperature is 450 K and the density is 1.26 g/cm^3. Six of the chains have a regular repeating sequence of diads, $(MR)_x$, $(MMR)_x$, $(MRR)_x$, $(MRRR)_x$, where M and R denote *meso* and *racemo* diads, respectively, along with sPVC and isotactic PVC (iPVC). Each sequence is truncated as necessary to produce a chain with 50 monomer units. The remaining melt is composed of chains that have a Bernoullian sequence of diads and a 50:50 ratio of M and R. This chain represents aPVC. The atactic chain and $(MR)_x$ have the same stereochemical composition but different stereochemical sequences.

Table 1. Probability for a *Racemo* Diad, Time (MCS/10^5) for Mean-Square Displacement of the Center of Mass Equal to the Mean-Square Radius of Gyration, and Average Energy per Bead (kJ/mol) in the One-Component Melts

chain	p_R	τ	E_{total}	E_{RIS}	E_{LJ}
iPVC	0.00	5	−0.22 ± 0.06	6.48 ± 0.03	−6.70 ± 0.04
$(MMR)_x$	0.33	17	−0.56 ± 0.08	6.05 ± 0.06	−6.61 ± 0.03
aPVC	0.50	18	−0.48 ± 0.08	6.10 ± 0.06	−6.69 ± 0.05
$(MR)_x$	0.50	19	−0.36 ± 0.13	6.03 ± 0.09	−6.40 ± 0.08
$(MRR)_x$	0.67	49	−0.91 ± 0.20	5.76 ± 0.18	−6.68 ± 0.08
$(MRRR)_x$	0.75	90	−1.21 ± 0.26	5.65 ± 0.16	−6.86 ± 0.14
sPVC	1.00	433	−4.07 ± 0.44	4.61 ± 0.22	−8.69 ± 0.29

The stereochemical composition has a strong influence on the dynamic and energetic behavior of the melts, as shown in Table 1. The average time, τ, for a mean-square displacement of the center of mass that is equal to the mean-square radius of gyration is shown in the third column. This time increases as the syndiotactic character of the chain increases. It is 2 orders of magnitude larger for sPVC than for iPVC. This change in mobility is accompanied by changes in the average energy and in the two components of this energy, as shown in the last three columns of Table 1. The molecular origin of these effects in the present simulation of PVC is similar to the origin of the miscibility effects in the PP melts, which were studied earlier.[15] In both polymers, sequences of bonds in *trans* states can easily form in subchains composed of *racemo* diads. This tendency is stronger in PVC than in PP. At 450 K, the RIS models yield probabilities for two consecutive bonds in *trans* states of 0.91 for sPVC and 0.45 for sPP. For comparison, this probability is 0.31 for polyethylene at the same temperature. If sequences of bonds in *trans* states form in two subchains that are collinear, and in a third shell occupancy with respect to one another, these *all-trans* sequences are longer lived than they would be if they were uncorrelated with one another. The intermolecular interaction of these two extended and aligned segments, separated from one another by a distance near the minimum in the Lennard-Jones potential describing the interaction of two monomer units, provides a slightly "sticky" interaction. This interaction reduces the mobility of the chain in the simulation and lowers the LJ contribution to the total energy of the system. There is also a change in the RIS contribution to the total energy, due to the shift in the population of rotational isomeric states toward the value characteristic of the *trans* state. All of these effects, which were observed previously in simulations of PP,[15] are apparent in the last four columns of Table 1.

The special character of the sPVC melt is also apparent in the intermolecular pair correlation functions (pcf). On the high coordination lattice, a discrete pcf, $g_{AA}(i)$, can be defined as in eq 1.

$$g_{AA}(i) = \frac{1}{(10i^2 + 2)V_A}\sum n_{AA}(i) \qquad (1)$$

The concentration of species A in the system is denoted by V_A, $n_{AA}(i)$ is the number occupancy of A in the ith

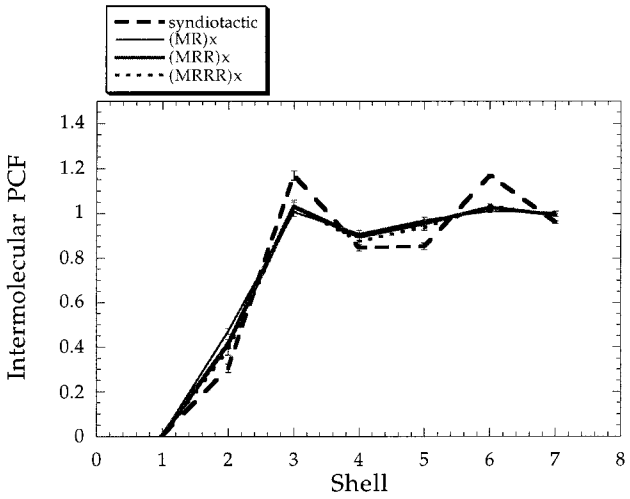

Figure 1. Intermolecular pcfs for one-component melts of sPVC, $(MR)_x$, $(MRR)_x$, and $(MRRR)_x$ at 450 K and a density of 1.26 g/cm^3.

shell around another bead of A, and *i* indexes the shell number. Thus, the distance between two points in the simulation is quantified by the discrete shell number. For the special case of the intermolecular pcf, which is used here, the two monomers are members of different chains.

Intermolecular pcf for four of the one-component melts are depicted in Figure 1. The intermolecular pcfs for $(MR)_x$, $(MRR)_x$, and $(MRRR)_x$ are similar to one another, with each pcf showing very weak local maxima in the third and sixth shells and a weak local minimum in the fourth shell. These three pcfs are barely distinguishable from one another on the scale used in Figure 1. The remaining pcf, for sPVC, is easily distinguishable from the other three pcfs because of its stronger local maxima in the third and sixth shells and lower values of $g_{AA}(i)$ at the two intervening shells. In other words, the sPVC melt shows more evidence of a tendency for the formation of local "structure", as reflected by maxima in the intermolecular pcfs in the third and sixth shells, than is the case in the other three melts. Intermolecular pcfs for the remaining three melts studied, namely iPVC, aPVC, and $(MMR)_x$, are not depicted here, but they can be found in the Supporting Information. They are nearly identical with the intermolecular pcfs depicted in Figure 1 for $(MR)_x$, $(MRR)_x$, and $(MRRR)_x$. Thus, the syndiotactic stereochemical composition is unique for PVC with regard to a tendency for the formation of local structure in its melt, as detected by the intermolecular pcfs.

Two-Component Melts. Simulations were performed for 12 two-component melts, with each mixture containing pairs of chains from Table 1. Each simulation uses 10 chains of each type and is performed at a density of 1.24 g/cm^3 and a temperature of 450 K.

The time dependence of the tendency for demixing in the two-component melts can be monitored by following the intermolecular pcfs in the third shell, which is the location of the first maximum in the intermolecular pcfs for the one-component melts, as is shown in Figure 1. Four intermolecular pcfs are monitored. Two of these intermolecular pcfs, $g_{AA}(i)$ and $g_{BB}(i)$, are evaluated for monomer units of chains with the same stereochemical composition. A third intermolecular pcf, $g_{total}(i)$, is evaluated using all of the chains, without regard to their stereochemical composition. Finally, the intermolecular

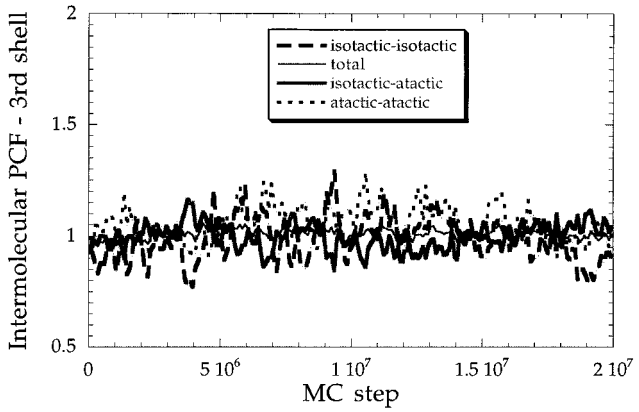

Figure 2. Values of the four intermolecular pcfs in the third shell for the equimolar melt of aPVC and iPVC at 450 K and 1.24 g/cm^3.

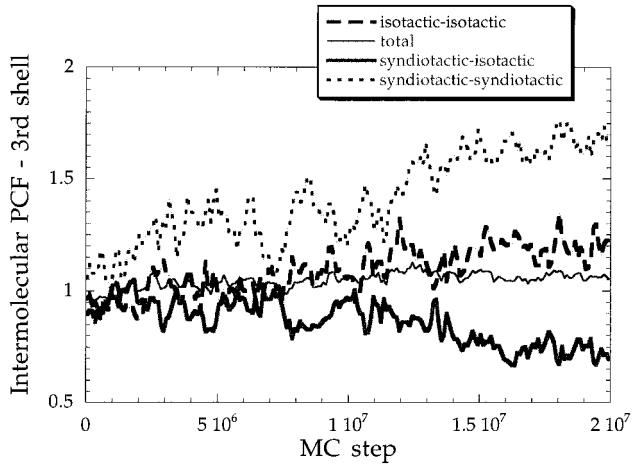

Figure 3. Values of the four intermolecular pcfs in the third shell for the equimolar melt of iPVC and sPVC at 450 K and 1.24 g/cm^3.

cross-correlation function, $g_{AB}(i)$, is evaluated using pairs of monomer from chains of different stereochemical composition. The two types of time dependencies observed are illustrated in Figures 2 and 3.

Figure 2 depicts the value of the four intermolecular pcfs in the third shell for the simulation of the equimolar mixture of iPVC and aPVC. Each of the four intermolecular $g(3)$ experiences oscillations about a value close to 1. There is no evidence of a systematic change in any of the $g(3)$ over 2×10^7 MCS, nor is there any evidence that any one of the $g(3)$ is distinguishable from the other three $g(3)$. This result is the one expected for a completely miscibile system, in which the two types of chains mix without regard for their differences in stereochemical composition.

A different type of behavior is depicted for the mixture of iPVC and sPVC in Figure 3. Here the values of $g(3)$ diverge from one another as the simulation progresses. The intermolecular cross-correlation decreases to values much smaller than 1, and the intermolecular pcf between chains of the same stereochemical composition increases to values significantly larger than 1, as time progresses. There is much less evidence for change in the remaining intermolecular g(3), which is evaluated for all chains in the system, without regard to their stereochemical composition, and remains in the vicinity of 1.0−1.1. This behavior is the result expected for a two-component melt that is on the verge of demixing.

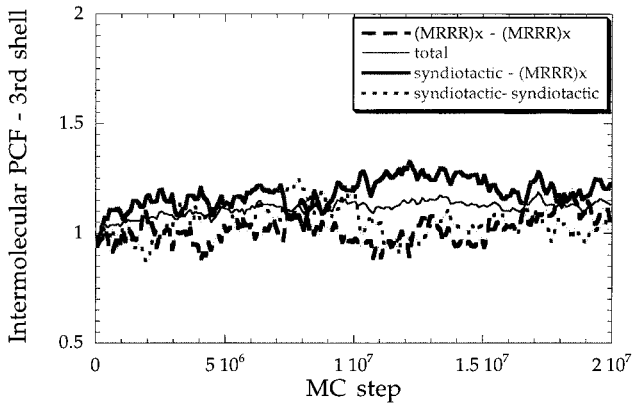

Figure 4. Values of the four intermolecular pcfs in the third shell for the equimolar melt of sPVC and $(MRRR)_x$ at 450 K and 1.24 g/cm^3.

Beads in each chain prefer to surround themselves with beads from other chains with the same stereochemical composition. The drive toward demixing has become obvious 1×10^7 MCS into the simulation, where the intermolecular cross-correlation $g(3)$ becomes obviously lower than the other three $g(3)$.

The behavior of the remaining 10 equimolar mixtures studied can be quickly summarized by citing their relationships to Figures 2 and 3. Six of the equimolar mixtures do not contain sPVC. All six of these mixtures exhibit intermolecular $g(3)$ with behavior similar to that depicted in Figure 2. These mixtures, $(MMR)_x$−iPVC, $(MMR)_x$−$(MR)_x$, $(MMR)_x$−aPVC, $(MRR)_x$−$(MRRR)_x$, $(MR)_x$−$(MRRR)_x$, and $(MMR)_x$−$(MRR)_x$, show no evidence of demixing. The data are not presented here but can be found in the Supporting Information.

The remaining four mixtures contain sPVC as one of the two components. Three of these four mixtures show the same type of evidence for demixing as can be seen in Figure 3. Demixing of sPVC from $(MR)_x$ becomes evident at nearly the same stage of the simulation as for sPVC−iPVC in Figure 3. Evidence of demixing is also generated, but at a slightly later state of the simulation, for sPVC and either aPVC or $(MMR)_x$. The data for these three systems can be found in the Supporting Information.

The data for the remaining two-component system shows behavior that is qualitatively different from that of the other 11 two-component melts studied. The time dependence of the intermolecular $g(3)$ for this system, the equimolar melt of sPVC and $(MRRR)_x$, is depicted in Figure 4. In this system, the intermolecular cross-correlation function grows to a size larger than the other three $g(3)$, and the two intermolecular $g(3)$ evaluated for chains with a particular stereochemical composition are tending to become smaller than the other two intermolecular $g(3)$. This behavior is the reverse of the result obtained in Figure 3 for the melt of sPVC and iPVC. It suggests the opposite of demixing, namely, the tendency for the formation of a weak intermolecular complex between syndiotactic PVC and $(MRRR)_x$, such that beads from each chain have a weak preference to surround themselves with beads from the other type of chain. Since $(MRRR)_x$ appears to be miscible with chains containing a higher content of *meso* diads, based on its behavior with $(MRR)_x$ and $(MR)_x$, it might serve as a compatabilizer for sPVC and PVC having stereochemical compositions more typical of this material, as it is usually prepared.

In principle, an energy of mixing could be calculated for each of the blends from the data in Table 1 and the average energy per bead in the two-component mixtures.

$$\Delta E_{\mathrm{mix}} = E_{\mathrm{AB}} - \frac{1}{2}(E_{\mathrm{A}} + E_{\mathrm{B}}) \qquad (2)$$

However, this process involves taking a small difference between two large numbers, and the uncertainties due to the fluctuations in each individual energy during the simulation accumulate to a larger value than ΔE_{mix} itself. For example, in the blend of iPVC and sPVC, the values of E_{A} and E_{B}, from Table 1, are -0.22 ± 0.06 and -4.07 ± 0.44 kJ/mol. The value of E_{AB}, averaged over the last half of the simulation for the two-component melt, is -2.02 ± 0.16 kJ/mol. Application of eq 2 gives an energy of mixing of 0.12 ± 0.41 kJ/mol, where the uncertainty dominates the average. For this reason, the energetic analysis of the blends is not pursued further here.

Summary

Intermolecular pcfs and average energies evaluated from simulations of one-component melts of PVC establish sPVC as being different from chains in which the fraction of *racemo* diads is 0.75 or smaller. This difference appears as a greater tendency for the formation of a local "structure", arising from intermolecular interaction of two or more subchains of *racemo* diads in which the C−C bonds adopt *trans* states. This behavior is qualitatively similar to the result obtained previously for sPP in the melt.

Equimolar two-component melts composed of PVC chains with different stereochemical composition are miscible, provided one of the components is not sPVC. All but one of the melt blends containing sPVC experience spontaneous demixing. The exception is provided by the melt blends of sPVC with $(MRRR)_x$. In this system, the intermolecular pcfs reveal a weak tendency for the formation of an intermolecular complex between the sPVC and $(MRRR)_x$. Since $(MRRR)_x$ is miscible with PVCs of typical stereochemical composition, the $(MRRR)_x$ may serve as a compatabilizer for sPVC and other PVCs in the melt.

Acknowledgment. This work was supported by Grant DMR0098321 from the Polymer Program at the National Science Foundation.

Supporting Information Available: Figure depicting intermolecular pcfs for the one-component melts of aPVC, iPVC, and $(MMR)_x$ and nine figures depicting the time dependence of the four intermolecular $g(3)$ for equimolar mixtures of $(MMR)_x$−iPVC, $(MMR)_x$−$(MR)_x$, $(MMR)_x$−$(MRRR)_x$, $(MRR)_x$−$(MRRR)_x$, $(MR)_x$−$(MRRR)_x$, $(MMR)_x$−$(MRR)_x$, and sPVC mixed with either aPVC, $(MR)_x$, or $(MMR)_x$. This material is available free of charge via the Internet at http://pubs.acs.org.

References and Notes

(1) Hay, J. N.; Biddlestone, F.; Walker, N. *Polymer* **1980**, *21*, 985.
(2) Walsh, D. J.; Higgins, J. S.; Druke, C. P.; McKeown, J. S. *Polymer* **1981**, *22*, 168.
(3) Guerrero, S. J.; Keller, A.; Soni, P. L.; Geil, P. H. *J. Macromol. Sci., Phys.* **1981**, *20*, 167.
(4) Komoroski, R. A.; Lehr, M. H.; Goldstein, J. H.; Long, R. C. *Macromolecules* **1992**, *25*, 3381.
(5) Ballard, D. G. H.; Burgess, A. N.; Dekoninck, J. M.; Roberts, E. A. *Polymer* **1987**, *28*, 3.

(6) Scherrenberg, R.; Reynaers, H.; Mortensen, K.; Vlak, W.; Gondard, C. *Macromolecules* **1993**, *26*, 3205.
(7) Henson, J. H. L.; Hybart, F. J. *J. Appl. Polym. Sci.* **1972**, *16*, 1653.
(8) Yano, S. *J. Appl. Polym. Sci.* **1977**, *21*, 2645.
(9) Wilkes, C. E. *Macromolecules* **1971**, *4*, 443.
(10) Ludovice, P. J.; Suter, U. W. In *Computational Modeling of Polymers*; Bicerano, J., Ed.; Marcel Dekker: New York: 1992; p 401.
(11) Lee, K.-J.; Mattice, W. L. *Comput. Polym. Sci.* **1992**, *2*, 55.
(12) Smith, G. D.; Jaffe, R. L.; Yoon, D. Y. *Macromolecules* **1993**, *26*, 298.
(13) Doruker, P.; Mattice, W. L. *Macromolecules* **1997**, *30*, 5520.
(14) Baschnagel, J.; Binder, K.; Doruker, P.; Gusev, A. A.; Hahn, O.; Kremer, K.; Mattice, W. L.; Müller-Plathe, F.; Murat, M.; Paul, W.; Santos, S.; Suter, U. W.; Tries, V. *Adv. Polym. Sci.* **2000**, *152*, 41.
(15) Clancy, T. C.; Pütz, M.; Weinhold, J. D.; Curro, J. G.; Mattice, W. L. *Macromolecules* **2000**, *33*, 9452.
(16) Lohse, D. J. *Polym. Eng. Sci.* **1986**, *26*, 1500.
(17) Thomann, R.; Kressler, J.; Setz, S.; Wang, C.; Mülhaupt, R. *Polymer* **1996**, *37*, 2627.
(18) Thomann, R.; Kressler, J.; Rudolf, B.; Mülhaupt, R. *Polymer* **1996**, *37*, 2635.
(19) Maier, R. D.; Thomann, R.; Kressler, J.; Mülhaupt, R.; Rudolf, B. *J. Polym. Sci., Part B* **1997**, *35*, 1135.
(20) Rapold, R. F.; Mattice, W. L. *J. Chem. Soc., Faraday Trans.* **1995**, *91*, 2435.
(21) Orwoll, R. A. In *Physical Properties of Polymer Handbook*; Mark, J. E., Ed.; American Institute of Physics: Woodbury, NY, 1996; p 81.
(22) Haliloglu, T.; Mattice, W. L. *J. Chem. Phys.* **1998**, *108*, 6989.
(23) Mattice, W. L.; Clancy, T. C. *Macromolecules* **1999**, *32*, 5444.
(24) Cho, J.; Mattice, W. L. *Macromolecules* **1997**, *30*, 637.
(25) Reid, R. C.; Prausnitz, J. M.; Poling, B. E. *The Properties of Gases and Liquids*, 4th ed.; McGraw-Hill: New York, 1987.
(26) Clancy, T. C.; Mattice, W. L. *J. Chem. Phys.* **2000**, *112*, 10049.

MA010462C